Adsorption (2017) 23:355–360
DOI 10.1007/s10450-017-9860-y

Effects of phosphoric acid activation on the nanopore structures of carbon xerogel/carbon nanotubes hybrids and their capacitance storage

Nady A. Fathy[1,2] · K. P. Annamalai[2] · Yousheng Tao[2,3]

Received: 30 June 2016 / Revised: 2 January 2017 / Accepted: 5 January 2017 / Published online: 13 January 2017

Abstract This paper aimed to study the electrochemical capacitance behaviors in relation to the nanopore structures of three carbon materials, which were prepared under different conditions and named as carbon xerogels (CXs), carbon xerogels/carbon nanotubes hybrids (CXs/CNTs) and activated carbon xerogels/carbon nanotubes hybrids (aCXs/CNTs). Field emission scanning electron microscopy showed the growth of CNTs on the CXs surface in the CXs/CNTs hybrids. Nitrogen physisorption measurements at 77 K indicated a decrease in the specific surface area and the total pore volume of micropores and mesopores after decorating the CXs surface with CNTs, however an increase after activation with phosphoric acid at 973 K for 180 min. Because of the combination of CNTs and phosphoric acid activation, electrochemical capacitance increased in the order of CXs < CXs/CNTs < aCXs/CNTs and it delivered maximum capacitance of 151 F g^{-1} at 2.5 A g^{-1} in 1 M H_2SO_4.

Keywords Synthesis · Carbon xerogel · Carbon nanotube · Nitrogen adsorption · Micropore · Mesopore · Capacitance

✉ Yousheng Tao
taoys@tom.com

[1] Physical Chemistry Department, National Research Centre, 33 El Buhouth Street, Dokki, P.O. 12622 Cairo, Egypt

[2] CAS Key Laboratory of Design and Assembly of Functional Nanostructures, Haixi Institutes, Chinese Academy of Sciences (CAS), Fuzhou 350002, China

[3] R&D Center of Saline Lake and Epithermal Deposits, Chinese Academy of Geological Sciences, Beijing 100037, China

1 Introduction

Nanoporous carbon materials such as activated carbon, carbon aerogels (CAs) or carbon xerogels (CXs) and carbon nanotubes (CNTs) used as capacitor electrodes are of considerable interest due to their high conductivity, large specific surface area, low density, superior chemical and mechanical stability (Frackowiak et al. 2001; Fischer et al. 1997; Halama et al. 2010; Mezzavilla et al. 2012; Tao et al. 2008; Portet et al. 2005). CNTs have been intensively studied as electrodes in supercapacitors (Volder et al. 2013; Iijima et al. 1991), but are currently limited because of their low specific capacitance (Kim et al. 2012). Recently carbon-based nanocomposites or nanohybrids were found to enhance capacitance storage, superior to the individual component alone (Annamalai et al. 2015). It was reported that the incorporation of CNTs into CAs or CXs during sol–gel process made the composites useful for electrochemical capacitor application (Bordjiba et al. 2008; Worsley et al. 2008). Such materials have characteristics such as (i) high specific capacitance, (ii) high conductivity and (iii) good thermal and chemical stability; however there is a lack of intensive research about nanopore structures relative to the capacitance storage (Chidembo et al. 2010).

In this study, nickel oxide loaded on CXs was used as a catalyst for direct growth of CNTs on CXs to obtain CXs/CNTs hybrids with chemical vapor deposition (CVD) technique using camphor as a botanical carbon precursor. In order to obtain large nanoporosity, the as-grown CXs/CNTs were activated with phosphoric acid and the products were denoted as aCXs/CNTs. The nanopore structures of samples were characterized with N_2 adsorption at 77 K. The electrochemical capacitance behaviors in relation to the textural properties of aCXs/CNTs was compared with that of CXs and CXs/CNTs.

2 Experimental

2.1 Sample preparation

The resorcinol–formaldehyde polymer xerogels were pyrolyzed to produce CXs, based on a procedure described elsewhere (Fathy et al. 2016). The CNTs were grown using a CVD method in a stainless steel tube with the diameter 32 mm and length 80 mm, which was placed in horizontally two electric furnaces. Inexpensive and nontoxic commercial camphor was used as hydrocarbon source, while CXs supported nickel nanoparticles were used as catalysts. The camphor in an alumina boat was kept inside the first furnace. When camphor was heated at 523 K to get gas phase reaction mixture, the temperature of 2nd furnace with CXs in an alumina boat was set to 1123 K for growing CNTs on CXs for 60 min, where the vapors liberated from camphor were moved to the 2nd furnace with high temperature by a N_2 gas flow. The resulting products of CXs/CNTs hybrids were obtained after the two furnaces were switched off. Finally, a desired amount of CXs/CNTs was impregnated 50 v/v% phosphoric acid followed by stirring overnight and then dried in an air-oven at 353 K for several hours. After that, the impregnated samples were subjected to activation at 973 K for 3 h under flowing of N_2 gas. After cooling, the samples were washed with distilled water, dried at 373 K and then aCXs/CNTs was obtained.

2.2 Characterizations

The morphologies of samples were studied with field-emission scanning electron spectroscope (FE-SEM) (JSM-6700, JEOL) and transmission scanning electron spectroscope (TEM) (TecnaiF20, Philips). N_2 adsorption at 77 K (ASAP 2010, Micromeritics) was employed for the determination of the pore structure parameters. The Saito–Foley method and the Barrett–Joyner–Halenda (BJH) method were used to analyze the micropores and mesopores of samples, respectively (Saito et al. 1991; Barrett et al. 1951). To evaluate the electrochemical characteristics of the materials as electrode in aqueous systems, the cyclic voltammetry (CV) and galvanostatic charge–discharge (GCD) measurements were performed on a CHI 660E electrochemical workstation (Shanghai CH Instruments) with typical three-electrode measurement, where active materials coated Pt mesh, Ag/AgCl and Pt foil were used as working, reference and counter electrodes, respectively. The working electrode was prepared using test sample and polyvinylidene difluoride (PVDF) binder, which were uniformly mixed in the weight ratio of 95:5 and were made as a slurry using N-methyl-2-pyrrolidone. The slurry was coated on Pt mesh electrode, dried in an air oven at 343 K overnight. The mass loading was determined to be 0.8 mg cm^{-2} by weighing the Pt mesh before and after coating active materials. Electrochemical tests were performed at room temperature in 1 M H_2SO_4. The CVs were measured in the potential range of −0.1 to 0.9 V with both the three- and two-electrode cell configuration.

3 Results and discussion

Figure 1 presented the FE-SEM images of CXs, CXs/CNTs and aCXs/CNTs and TEM image of aCXs/CNTs samples, showing an obvious difference in the morphologies of the samples. As shown in Fig. 1a, CXs were composed of nano-sized carbon spherical particles, which interconnected to form irregular three-dimensional network-structure. The pores or cavities were formed among the carbon particles. In Fig. 1b, the growth of CNTs on the CXs surface was found in the CXs/CNTs nanohybrids. Chemical activation for CXs/CNTs with phosphoric acid yielded the hybrids of highly nanoporous structures, as depicted in Fig. 1c. The formation of micro- and mesopores in the network of aCXs/CNTs nanohybrids were further evidenced with TEM observation, as illustrated in Fig. 1d.

Nitrogen adsorption/desorption isotherms at 77 K on all samples were shown in Fig. 2a. Although all samples showed the uptakes in N_2 adsorption below $P/P_0 = 0.02$, indicating micropore filling, their microporosities were quite different from one to another (Gregg et al. 1991; Sing et al. 2008). The BET specific surface area of CXs significantly decreased from 330 to 95 $m^2\ g^{-1}$ after the in-situ growth of CNTs, while it increased to 215 $m^2\ g^{-1}$ upon phosphoric acid activation. In comparison with CXs/CNTs, aCXs/CNTs had much large total surface area and pore volume, which was attributed to the formation of new micro and mesopores. Comparing both the shapes and amount of all N_2 adsorption isotherms at $P/P_0 > 0.2$, one can find the enhancement of mesopore fractions in the porous texture of aCX/CNTs. It should be attributed to two possible reasons: (i) phosphoric acid activation created mesopores in CXs subtract and (ii) the interspacing among nanotubes contributed to a number of mesopores (as well as macropores). The surface areas and porosity data for the samples were summarized in Table 1. The CVD technique yielded ~16.3 wt% of CNTs, which was in agreement with earlier work about the synthesis of CNTs on the surface of activated carbon fiber (Hsieh et al. 2009).

To investigate the relationship between pore structures and capacitance storage performance, the samples were tested as a supercapacitor electrode. Figure 2b showed the comparative cyclic voltammograms of the CXs, CXs/CNTs and aCXs/CNTs at room temperature in 1 M H_2SO_4 at 25 mV s^{-1} scan rate. The broad quasi-rectangular curves of all samples suggested nearly equal quantities of current

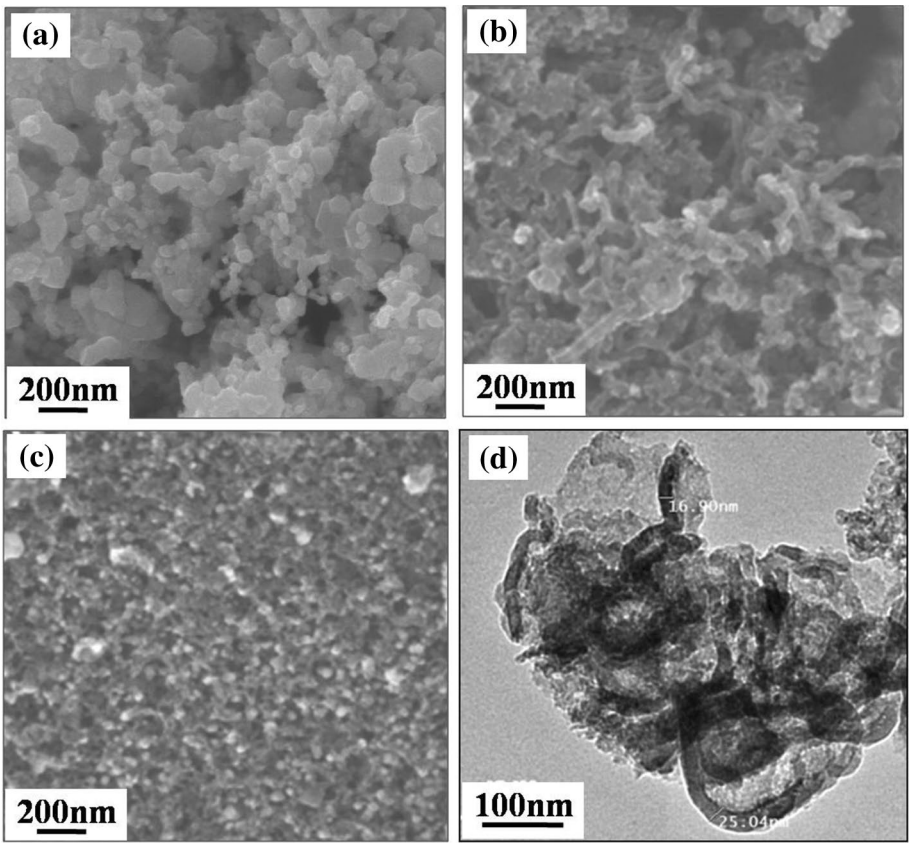

Fig. 1 FE-SEM images of **a** CXs, **b** CXs/CNTs, **c** aCXs/CNTs and TEM images of **d** aCXs/CNTs samples

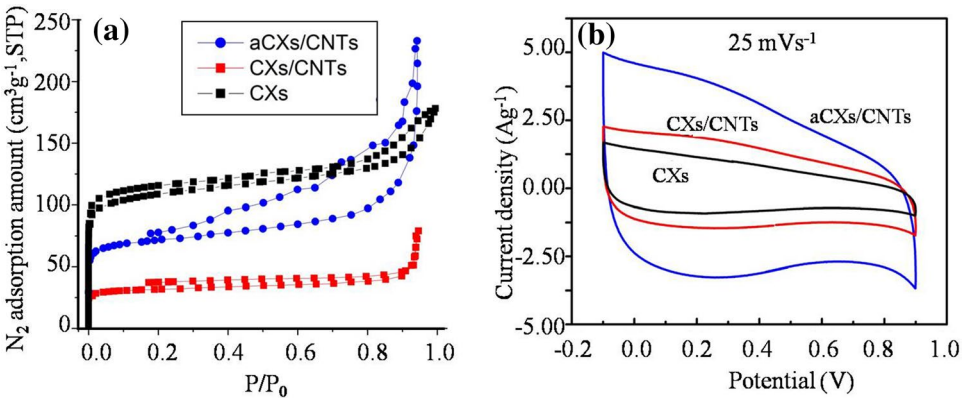

Fig. 2 **a** N_2 adsorption and desorption isotherms at 77 K on CXs, CXs/CNTs and aCXs/CNTs, **b** the comparative CV curves of CXs, CXs/CNTs and aCXs/CNTs in 1 M H_2SO_4 at 25 mV s^{-1} scan rate

Table 1 Surface areas and porosity data for the samples

Sample	S_{BET} (m^2 g^{-1})	Micropore volume (cm^3 g^{-1})	Mesopore volume (cm^3 g^{-1})	Mesopore width (nm)	Micropore width (nm)
CXs	330	0.17	0.11	2–20	0.6–1.6
CXs/CNTs	95	0.05	0.07	25–50	0.6–1.9
aCXs/CNTs	215	0.11	0.25	2–4, 30–50	1.3–2.0

necessary to charge and discharge each capacitor over the potential range of −0.1 to 0.9 V. Because CNTs provided more accessible active sites for transferring the protons and hydration ions inside the electrochemical cell and because CNTs increased the conductivity of the whole matrixes of both CXs/CNTs and aCXs/CNTs, both of them showed an

obvious enhancement of capacitance storage in comparison with CXs.

The CV curves of aCXs/CNTs from 10 to 200 mV s^{-1} were shown in Fig. 3a. The insignificant shift in the positive and negative region upon increasing the scan rate illustrated the mesopores shortened the electrolyte ion path. The specific capacitances of both CXs/CNTs and aCXs/CNTs determined from CV curves were displayed in Fig. 3b. aCXs/CNTs had the maximum capacitance of 132 F g^{-1} delivered at 10 mV s^{-1} scan rate, which was 2.5 times higher than that of CXs/CNTs. Such a big enhancement of capacitance was mainly attributed to phosphoric acid activation, which developed many micro- and mesopores and enhanced the pesudocapactive behavior to some extent at the surface of the materials (Weng et al. 2001). Further increasing the scan rate, capacitance gradually dropped. It was mainly because upon fast scan rate electrolyte ions were unable to enter into most of the pores on short time interval (Zhang et al. 2009; Hulicova-Jurcakova et al. 2009). Because of less exploitation of pores at high scan rate, it resulted in 62% of capacitance retained at high scan rate of 200 mV s^{-1}. The CV measurements were also carried out in 2-electrode cell at the same potential range. Single electrode capacitance was highly reliable with 3-electrode test results. It also showed EDLC curves from the low to high scan rate in 1.0 M H_2SO_4.

The quasi-EDLC-type capacitive behavior was mainly derived from phosphoric acid activation. XPS core level spectra (not shown here) confirmed the incorporated P and its functional groups on carbon nanostructures. Two peaks were identified in P 2p core level spectra, in which the high intense peak at the binding energy of 134 eV was corresponding to C–O–PO_3 and low intense peak at 132.6 eV was due to P-doping into the carbons. It was clear that phosphoric acid activation primarily induced the nanoporosity and also gave minimal P-doping in the carbon nanostructures, which increased the capacitance storage competence through favorable mass transportation and induced pseudocapacitance, respectively. The results agreed with previously reported phosphoric acid based P-doped graphene, in which the presence of functional groups and heteroatom contributed in the form of pseudocapacitance to the specific capacitance (Karthika et al. 2013).

We further studied the electrochemical performance of the materials with GCD measurements at different current densities. Figure 4a showed the nearly identical triangular-type charge–discharge curves obtained throughout the current densites, indicating that current material was dominated by the mechanism of electric double layer capacitor (EDLC). The specific capacitance upon increasing current density was determined and shown in Fig. 4b. It delivered maximum specific capacitance of 151 F g^{-1} at 2.5 A g^{-1}, much higher than that of CXs/CNTs. While increasing the current density to 15 A g^{-1}, aCX/CNTs still exhibited 70% of its original capacitance. Such a high capacitance retention at high current density was mainly because CNTs in the hybrids decreased the ohmic resistance and what is more, further chemical activation developed a lot of nanopores accessible to electrolyte and increased wettability on the electrode–electrolyte interface. Hence, in-situ grown CNTs and phosphoric acid activation considerably synergized the capacitance storage ability of carbon xerogel materials.

4 Conclusions

We synthesized aCXs/CNTs hybrids with CNTs CVD-grown in situ on CXs using camphor as precursor and then chemically activated them with phosphoric acid. The nanoporosity of CXs significantly decreased after decoration

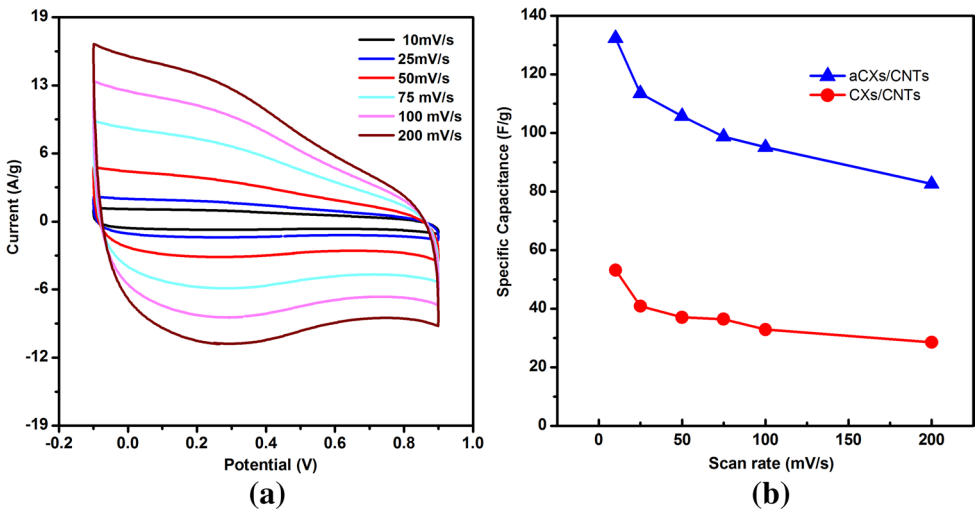

Fig. 3 **a** Cyclic voltammetry curves of aCXs/CNTs from 10 to 200 mV s^{-1} scan rate, **b** specific capacitance of aCXs/CNT versus scan rate in 1 M H_2SO_4 (that of CXs/CNTs was included for comparison purpose)

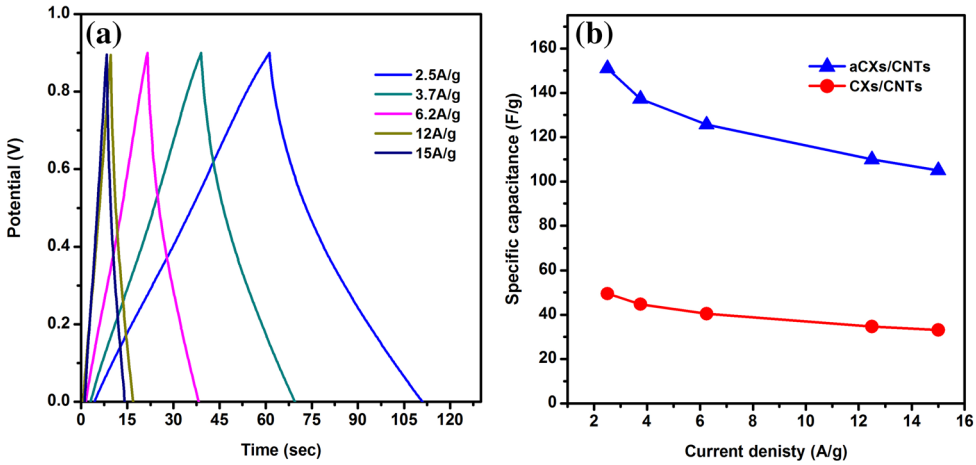

Fig. 4 **a** Galvanostatic charge–discharge measurements from 2.5 to 15 A g^{-1} in 1 M H_2SO_4, **b** specific capacitance versus current density for aCXs/CNTs. For comparison purpose, specific capacitance versus current density for CXs/CNTs was also included in **b**

with CNTs, while it increased upon phosphoric acid activation. It was evidenced the enhancement of mesopore fractions in the porous texture of aCX/CNTs. The materials showed electrochemical behavior superior to that of CXs and CXs/CNTs. aCX/CNTs exhibited highest specific capacitance of 151 F g^{-1} at a current density of 2.5 A g^{-1}, much higher than that of CXs and CXs/CNTs. The results revealed that CNTs grown in situ and phosphoric acid activation considerably increased electrochemical capacitance storage ability of carbon xerogel materials, promising for the applications in supercapacitors.

Acknowledgements This work was supported by the National Natural Science Foundation of China (21273236) and by Science and Technology Planning Projects of Fujian Province of China (2014H2008, 2015I0008 and 2014H4006). NAF and KPA acknowledge the post-doctorial research programs. YT acknowledges the support of both "100 Talents" program of the CAS and "100 Talents" program of Fujian Province, China.

References

Annamalai, K.P., Gao, J., Liu, L., Mei, J., Lau, W., Tao, Y.: Nanoporous graphene/single wall carbon nanohorn heterostructures with enhanced capacitance. J. Mater. Chem. A **3**, 11740–11744 (2015)

Barrett, E.P., Joyner, L.G., Halenda, P.P.: The determination of pore volume and area distributions in porous substances. I. Computations from nitrogen isotherms. J. Am. Chem. Soc. **73**(1), 373–380 (1951)

Bordjiba, T., Mohamedi, M., Dao, L.H.: Charge storage mechanism of binderless nanocomposite electrodes formed by dispersion of CNTs and carbon aerogels. J. Electrochem. Soc. **155**(2), A115–A124 (2008)

Chidembo, A.T., Ozoemena, K.I.: Electrochemical capacitive behaviour of multiwalled carbon nanotubes modified with electropolymeric films of nickel tetraaminophthalocyanine. Electroanalysis **22**(21), 2529–2535 (2010)

De Volder, M.F.L., Tawfick, S.H., Baughman, R.H., Hart, A.J.: Carbon nanotubes: present and future commercial applications. Science **339**(6119), 535–539 (2013)

Fathy, N.A., Attia, A.A., Hegazi, B.: Nanostructured activated carbon xerogels for removal of methomyl pesticide. Desalin. Water Treat. **57**(21), 9957–9970 (2016)

Fischer, U., Saliger, R., Bock, V., Petricevic, R., Fricke, J.: Carbon aerogels as electrode material in supercapacitors. J. Porous Mater. **4**(4), 281–285 (1997)

Frackowiak, E., Béguin, F.: Carbon materials for the electrochemical storage of energy in capacitors. Carbon **39**(6), 937–950 (2001)

Gregg, S.J., Sing, K.S.W.: Adsorption, Surface Area and Porosity. Academic Press, London (1991)

Halama, A., Szubzda, B., Pasciak, G.: Carbon aerogels as electrode material for electrical double layer supercapacitors—synthesis and properties. Electrochim. Acta. **55**(25), 7501–7505 (2010)

Hsieh, C.-T., Chen, W.-Y., Lin, J.-H.: Synthesis of carbon nanotubes on carbon fabric for use as electrochemical capacitor. Microporous Mesoporous Mater. **122**(1–3), 155–159 (2009)

Hulicova-Jurcakova, D., Seredych, M., Lu, G.Q., Kodiweera, N.K.A.C., Stallworth, P.E., Greenbaum, S., Bandosz, T.J.: Effect of surface phosphorus functionalities of activated carbons containing oxygen and nitrogen on electrochemical capacitance. Carbon **47**(6), 1576–1584 (2009)

Iijima, S.: Helical microtubules of graphitic carbon. Nature **354**(6348), 56–58 (1991)

Karthika, P., Rajalakshmi, N., Dhathathreyan, K.S.: Phosphorus-doped exfoliated graphene for supercapacitor electrodes. J. Nanosci. Nanotechnol. **13**, 1746–1751 (2013)

Kim, K.-S., Park, S.-J.: Synthesis and high electrochemical capacitance of N-doped microporous carbon/carbon nanotubes for supercapacitor. J. Electroanal. Chem. **673**, 58–64 (2012)

Mezzavilla, S., Zanella, C., Aravind, P.R., Della Volpe, C., Sorarù, G.D.: Carbon xerogels as electrodes for supercapacitors. The influence of the catalyst concentration on the microstructure and on the electrochemical properties. J. Mater. Sci. **47**(20), 7175–7180 (2012)

Portet, C., Taberna, P.L., Simon, P., Flahaut, E.: Influence of carbon nanotubes addition on carbon–carbon supercapacitor performances in organic electrolyte. J. Power Sources **139**(1–2), 371–378 (2005)

Saito, A., Foley, H.C.: Curvature and parametric sensitivity in models for adsorption in micropores. AIChE J. **37**, 429–436 (1991)

Sing, K.S.W., Everett, D.H., Haul, R.A.W., Moscou, L., Pierotti, R.A., Rouquerol, J., Siemieniewska, T.: Reporting physisorption data for gas/solid systems. In: Ertl, G., Knozinger, H., Weitkamp, J. (eds.) Handbook of Heterogeneous Catalysis. Wiley, New York (2008)

Tao, Y., Endo, M., Ohsawa, R., Kanoh, H., Kaneko, K.: High capacitance carbon-based xerogel film produced without critical drying. Appl. Phys. Lett. **93**(19), 193112 (2008)

Weng, T.-C., Teng, H.: Characterization of high porosity carbon electrodes derived from mesophase pitch for electric double-layer capacitors. J. Electrochem. Soc. **148**(4), A368–A373 (2001)

Worsley, M.A., Satcher, J.H., Baumann, T.F.: Synthesis and characterization of monolithic carbon aerogel nanocomposites containing double-walled carbon nanotubes. Langmuir **24**(17), 9763–9766 (2008)

Zhang, Y., Feng, H., Wu, X., Wang, L., Zhang, A., Xia, T., Dong, H., Li, X., Zhang, L.: Progress of electrochemical capacitor electrode materials: a review. Int. J. Hydrog. Energy **34**(11), 4889–4899 (2009)